

Received 12 June 2023, accepted 22 June 2023, date of publication 26 June 2023, date of current version 11 July 2023.

Digital Object Identifier 10.1109/ACCESS.2023.3289511

RESEARCH ARTICLE

Thyroid Detection and Classification Using DNN Based on Hybrid Meta-Heuristic and LSTM Technique

E. MOHAN¹, P. SARAVANAN², BALAJI NATARAJAN³, S. V. ASWIN KUMER⁴,
G. SAMBASIVAM⁵, (Member, IEEE), G. PRABU KANNA⁶, AND VAIBHAV BHUSHAN TYAGI⁷

¹Department of ECE, Saveetha School of Engineering, SIMATS, Chennai, Tamil Nadu 602105, India

²Department of Computing Technologies, School of Computing, SRM Institute of Science and Technology, Kattankulathur, Chennai, Tamil Nadu 603203, India

³Department of Computer Science and Engineering, Sri Venkateshwarra College of Engineering and Technology, Ariyur, Puducherry 605102, India

⁴Department of Electronics and Communication Engineering, Koneru Lakshmaiah Education Foundation, Vaddeswaram, Andhra Pradesh 522302, India

⁵School of Computing and Data Science, Xiamen University Malaysia, Sepang, Selangor 43900, Malaysia

⁶School of Computing Science and Engineering, VIT Bhopal University, Kothri Kalan, Sehore, Madhya Pradesh 466114, India

⁷Faculty of Engineering, ISBAT University, Kampala, Uganda

Corresponding author: Vaibhav Bhushan Tyagi (tyagi.fict@isbatuniversity.com)

ABSTRACT In the field of medical research, prediction, as well as diagnosis of thyroid disease, is a major cause that is a challenging onset axiom. In metabolism regulation, thyroid hormone secretions play a significant role. Two frequent thyroid diseases are hypothyroidism and hyperthyroidism that release the hormones like the thyroid, which regulate the body's metabolism rate. For analytics, the approach of data cleansing is utilized to analyze enough primitive data, which demonstrates the patients' risk. Deep Neural Networks (DNN) is the most vital as well as efficient technology, which predict the disorder of thyroid. To avoid the errors of human, the evaluation of manual process consumes expertise domain as well as time. To detect disease, a novel Long Short-Term Memory based Convolution Neural Network (LSTM-CNN) is utilized with occurrence area Vgg-19. For selecting the feature, the approach of bias field correction is integrated with the hybrid optimization technique i.e., Black Widow Optimization as well as Mayfly Optimization Approach (HBWO-MOA), also for classifying the disease the LSTM as well as Vgg-19 of Deep Learning (DL) is presented. From DDTI dataset image of ultrasound, the disease of thyroid prediction as well as classification is efficiency. This analysis shown that the proposed technology is accurate than the convolutional methodology. When compared to existing prediction techniques i.e., AlexNet-LSTM, ResNet-LSTM, Vgg16-LSTM, the proposed approach of Vgg-19-LSTM's precision, sensitivity, accuracy, recalls as well as F1_score is effective.

INDEX TERMS Classification, HMOA-BWO, LSTM, pre-processing, segmentation, Vgg-19.

I. INTRODUCTION

In the industry of healthcare, computational biology advances are being utilized for storing the collection of patient's data, which predict the medical diseases. A variety of techniques are accessible for early disease diagnosis. For analyzing the disease, the intelligent applications i.e., the information of medical technology are not accessible to collect the required sets of data [1], [2]. However, in recent days there is a

The associate editor coordinating the review of this manuscript and approving it for publication was Sangsoon Lim^{id}.

technology named as Machine Learning (ML) optimization, which plays a vital contribution for predicting & solving non-linear as well as complex issues. The features that can be chosen in any approach of disease detection, which classify easily in healthy persons, are emphasized as much as possible from multiple datasets. Instead, a healthy person may be exposed to unnecessary treatment because of misidentification. As a result, the accuracy of prediction any diseases along with thyroid is highest concern [3], [4], [5], [6].

In the neck, an endocrine gland is also known as the thyroid gland. It grows beneath the Adam's apple in the lower

part of the human neck, which aids in the thyroid secretion hormones, which affects the synthesis of protein as well as metabolism rate [7]. In the body, hormones of thyroid are useful for metabolism control in various ways, including how quickly the heart beats and the calories are burned. The production of thyroid gland aids in the control of the body's metabolism. Triiodothyronine known as T3 & levothyroxine known as T4 are the thyroid hormones, which actively secrete in Thyroid glands. These hormones are essential in the fabrication, as well as in the overall supervision construction, to regulate the body's temperature. T4 otherwise known as thyroxine as well as T3 are the two active hormones normally produced by the glands of thyroid. Throughout the body, storage of energy, regulation of temperature, transmissions, as well as management of protein are significant by these hormones. Iodine is regarded as a major building block of thyroid glands, which is compromised in a few specific concerns that are extremely common, for these two thyroid hormones, namely T3 as well as T4 [8], [9], [10], [11]. Thyroid hormone deficiency contributes to hypothyroidism, while excess thyroid hormones contribute to hyperthyroidism. Underactive thyroids as well as hyperthyroidism are the caused by various disorders. Medication comes in a variety of forms. Thyroid surgery exposes patients to deficiency of iodine, enzymelack, ionizing radiation, as well as tenderness of ongoing thyroid, which produce thyroid hormones [12].

Diagnosing of different thyroid diseases are now recognized by utilizing the technology known as ultrasound image. The patient's Thyroid Ultrasound Standard Plane (TUSP) is collected by utilizing the device known as ultrasound in the clinical diagnosis, and then the Transverse Plane of Thyroid Isthmus (TPTI) is employed to convert the TUSP image manually, the Downside of the Transverse Plane of The Right Part of Thyroid (DTPRT), the Longitudinal Plane of Thyroid Isthmus (LPTI), the Upside of the Transverse Plane of the Right Part of Thyroid (UTPRT), the Longitudinal Plane of the Left Part of Thyroid (LPLT), the Mid-size of the Transverse Plane of the Left Part of Thyroid (MTPLT), the Mid-side of the Transverse Plane of the Right Part of Thyroid (MTPRT), as well as ten categories are evaluated by the physician after the TUSP images [13], [14]. In general, the approach of Deep Learning (DL) is categorized into two phases: initially, the methodology i.e., Deep Neural Network (DNN) is utilized for training the sample images as well as extract the deepest features, and finally the trained neural network is employed to either classify or identify the sample images [15].

For predicting as well as classifying the thyroid diseases, the approach of CNN-LSTM is utilized in this research. To classify the disease, the model of CNN uses the base network known as Vgg-19. For reducing the computational complexity, Vgg-19-based LSTM is proposed. Also, it improves the accuracy of LSTM. To address these difficulties, a new lightweight model of Vgg-19-based LSTM is presented to provide efficient outcomes in temporal data processing and for learning the multi-sequence ultrasound images are more useful.

The following is how this paper is organized: Section IV describes the proposed research methodology; section V displays the parameter optimization, experimental settings, performance metrics, analysis results, as well as comparison. Also, it contains a brief discussion of disease diagnosis, and section 6 determines the conclusion as well as future work of presented technology.

II. RELATED WORK

In 2019, Liu et al. [16] have presented the automated nodules' classification as well as detection of ultrasound images by utilizing the specific task i.e., DL-based technology of CAD. Two process of CAD architecture was presented to detect nodules & learn features of pyramidal employing detection network of Multi-Scale Region at various scales of features. The prior knowledge of real nodules was estimated by the distributions of shape as well as size. The thyroid discrimination nodules' simulation was effective.

In 2019, Ma et al. [17] have developed the thyroid diagnosis utilizing the SPECT images with CNN optimization-based aided computer. The CNN's structure of DenseNet was trained as well as developed. The images of SPECT were accurate to diagnosis of thyroid diseases & its performance was superior to other conventional techniques.

In 2020, Song et al. [18] have introduced the images of ultrasound's feature cropping with CNN-based hybrid multi-branch to extract as well as classify the nodules of thyroid. To decrease the classification impact via a same kind of local features between malignant as well as benign images of thyroid nodule, a cropping of feature branch to the network was added for establishing the multi-cropping on batch feature maps. In both datasets of public as well as local, the methodology of proposed was outperformed & achieved accuracy of 96.13 %, precision of 93.24 %, recall of 97.18 %, as well as F1-measure of 95.17 %.

In 2020, Moussa et al. [19] have proposed a ResNet-50 based CNN technology from the approach of DL fine-tuning. In the images of ultrasound, the accuracy was enhanced to classify the nodules of thyroid. The analysis was processed utilizing the images of 814 ultrasound by the methodology of Vgg-19 to enhance the dramatically classification' effectiveness.

In 2020, Abdolali et al. [20] have developed the hyper-parameters of network as well as regularization of function loss with designed carefully by the network of unique DNN to enhance the detection without the steps of refinement based complex post-processing. Multi-Task model-based Mask of R-CNN technology was presented to frame the core of DL approach. Over the segmentation of prioritizes prediction method, a function of loss algorithm was developed. From the patients of 20, validation procedure was developed for 821 ultrasound frames. Nodules of different thyroid were detected by this presented technology. The detection of thyroid nodule was superior while comparing with the other approaches.

In 2020, Shankarlal et al. [21] have employed the detector of Kirsch's edge to enhance the images of thyroid with the pixels of edge region along with the Dual Tree Contourlet Transform (DTCT) to obtain the coefficients. The classifier of Co-Active Adaptive Neuro Expert System (CANFES) was utilized the features to form the transformed image of thyroid. Then, to segment the regions of tumor, the abnormal image of thyroid is segmented with the features of morphology. Finally, the segmented region of tumor was classified utilizing the approach of CNN to diagnosing the moderate, severe, as well as mild features.

In 2021, Hosseinzadeh et al. [22] have developed the diseases of thyroid from the reports of semantic utilizing the network of ANN to enhance the efficacy of diagnosis in the architecture of IoMT. During the process of training, the Multiple Multilayer Perceptron (MMLP) based ability of back-propagation error was presented to avoid over-fitting as well as enhance the generalization neural network feature. In the systems of IoMT, adaptive learning rate was compared with back-propagation in MMLP, accuracy of 4.6% was enhanced with the 99% of final accuracy.

In 2021, Namdeo et al. [23] have presented the new methodology of thyroid diagnosis including two phases i.e., extraction of feature as well as classification. Initially, Principal Component Analysis (PCA) as well as neighborhood-based gradient features was utilized to extract & sort the data features. The process of classification was also sorted. Finally, features of presented approach i.e., WF-CS was compared with PSO, FFA, CS, ABC, as well as proves the superiority for detecting the thyroid presence.

In 2021, Wan et al. [24] have introduced the unique imaging of CEUS dynamic for diagnosis the thyroid nodules with the Network of Hierarchical Temporal Attention (HiTAN) that enhance the classification of hierarchical nodules as well as learning the dynamic features into the deep framework. Gated Recurrent Units (GRUs) was modelled to diagnose the decompose dependency. The simulation analysis was enhancing the extensive efficacy of mechanism of hierarchical diagnosis as well as learning of dynamic patterns.

In 2021, Chu et al. [25] have presented the nodules of thyroid with the model of deep network-based mark-guided of ultrasound. To extract features of thyroid nodules with aim to consume time, detection of thyroid with U-Net was presented to diagnose the computer aided technology. The thyroid segmentation's accuracy was 3% higher than another convolutional network.

A. REVIEW

The previous part demonstrates the several techniques and frameworks utilized for thyroid disease classification. The discussed approaches are executed efficiently for predicting the thyroid disease even though some research gaps are stated as a future works. In [18] hybrid deep learning approach is utilized for the thyroid disease detection and

classification system. Even though the presented approach does not optimize the clip length. In [19] the dataset given for the presented detection and classification system does not includes variation in diseases. Therefore, this model is not suitable for the complex patterns. In [20] DNN was utilized for thyroid disease classification system, but it does not optimize the entire hyper parameters. Also, it is not applicable for edge cloud computing model. In [17] convolution neural network approach is utilized for the thyroid disease classification [26]. Since, for the minimization of the maximum likelihood loss function [27], the provided strategy does not provide improved results.

TABLE 1. Findings and challenges in existing works.

Authors [Citations]	FINDINGS	Challenges
In 2019, Liu et al., [16]	deep-learning-based CAD	Small dimension medical images are used.
In 2019, Maetal., [17]	CNN based SPECT images	Enhance the accuracy value is needed
In 2020, Song et al., [18]	hybrid multi-branch CNN	Not Optimize the Hyper Parameters.
In 2020, Moussa et al., [19]	Convolutional Neural Network model named resNet50.	Maximum Loss Function.
In 2020, Abdolaliet al., [20]	DNN	If the GPU Was Not Good, The Training Is Very Slow.
In 2020, Shankarlal et al., [21]	Dual Tree Contourlet Transform ANN in IoMT	Not Suitable for Complex Patterns Dataset.
In 2021, Hosseinzadehet al., [22]	WF-CS	Not Suitable to Personalized Health-Care Related Applications on Large Scale.
In 2021, Namdeoet al., [23]	hierarchical temporal attention network	Absence of hybridization algorithm.
In 2021, Wan et al., [24]	mark-guided ultrasound deep network	Not Suitable for More Than Three Different Complex Backgrounds.
In 2021, Chu et al., [25]	Deep learning-based classification	No prediction for trained data.
In 2022, S. K. Prabhakar et al., [29]	Deep learning is used	Reinforcement method adopted for implementation
In 2023, A. Sbrana et al., [32]		Suitable for hyperspectral images

III. PROPOSED METHODOLOGY

Classification of thyroid disease is critical for evaluating disease and making a handling decision [28] with respect to their classes. To detect thyroid disease, a variety of imaging techniques [29] are used. However, because of its higher image quality and the fact of relying on no ionizing radiation [30], MRI is commonly utilized. DL is a machine learning [31] subfield that has recently shown notable performance, specifically in classification and segmentation [32] issues. The proposed methodology diagram is shown in figure 1.

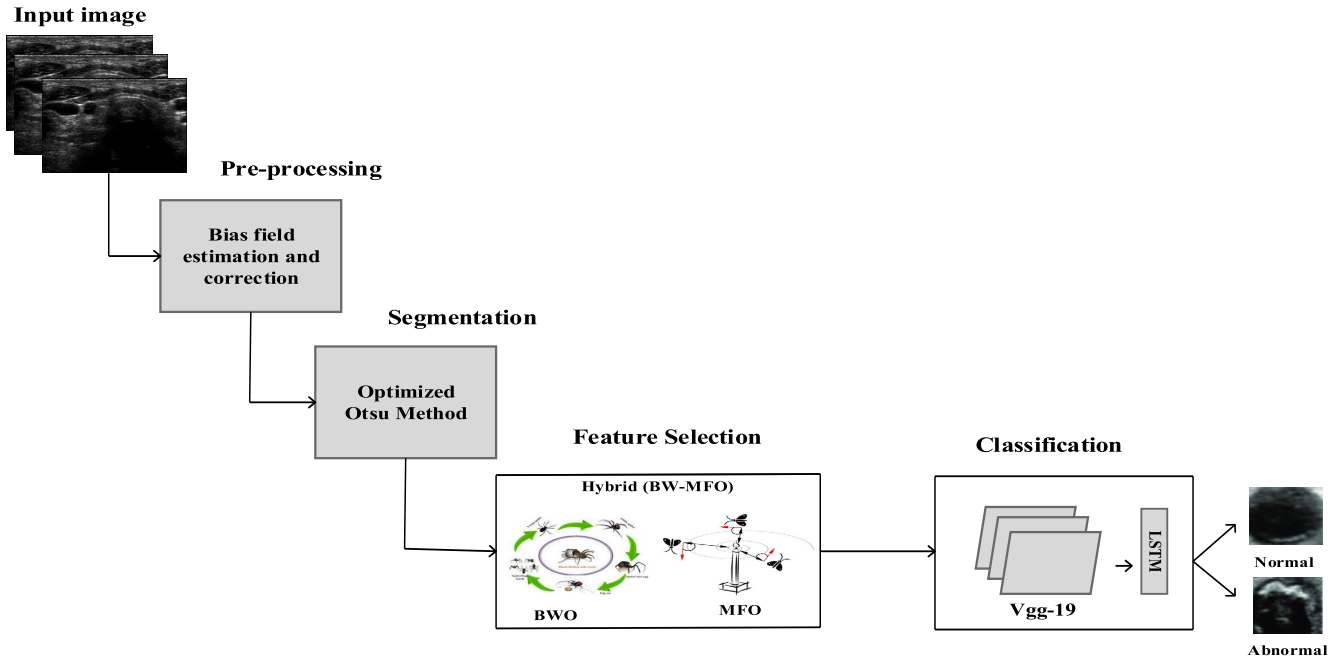


FIGURE 1. Overall flow of the proposed architecture.

In this paper, the thyroid disease prediction and classification approach include four phases such as pre-processing, segmentation, feature selection, and classification. Initially, the thyroid ultrasound images are collected, and the images are subjected to the pre-processing phase, in which bias field estimation and correction approaches [33] are performed. The bias field estimation and correction as well as smoothing is carried out to enhance the classification process. Next to the pre-processing phase, the image is segmented from the MRI image with the help of an optimized Otsu method segmentation. Once the image is segmentation process is completed then segmentation output goes to the feature selection process which merges the Black Widow optimization and Moth Flame Optimization Algorithm as a hybrid Meta Heuristic technique.

A. PRE-PROCESSING

Ultrasound images are affected in real-time applications because of vacillations of a coil in the magnetic field, which leads to intensity inhomogeneity and partial volume effect. Bias field estimation and correction are employed to solve this issue. The variation of grey level pixels of parallel tissues in the spatial domain is shown by the bias field, which detected as a multiplicative module of an ultrasound image. Hence, in this paper, bias field correction and smoothing approaches are employed to enhance the quality of classification results.

Assume P_t and X_0 are symbolizes as detected and actual images and n and b_{field} indicates the noise and bias field in a sample image written as in Eq. (1).

$$P_t = b_{field}X_0 + n \tag{1}$$

Furthermore, Gaussian filter $G(x, y)$ with the size of kernel as 3×3 is employed for image smoothing.

$$I_s(G(x, y)) = \frac{1}{2\pi\sigma^2} e^{-\frac{x^2+y^2}{2\sigma^2}} \tag{2}$$

σ represents standard deviation.

B. THYROID SEGMENTATION IMAGE TECHNIQUE UTILIZING OPTIMIZED OTSU'S APPROACH

Here, $I(X, Y)$ is the thyroid image along with levels of grey $0, 1 \dots \rho - 1$. Input imagery I candescribed as $F = \{f_0, f_1 \dots \dots f_{\rho} - 1\}$, where $f_0, f_1 \dots \dots f_{\rho} - 1$ represents frequency of every greyscale input image I .

Where, $N = \sum_{i=1}^{\rho} f_i$ is the total number of thyroid images in pixels.

Probability for i^{th} greyscale level is calculated as

$$Pr ob_i = \frac{f_i}{N}; Pr ob_i > 0, \sum Pr ob_i = 1 \tag{3}$$

This segmentation technique is an extension of Otsu's method. The segmentation method partitions the thyroid image to $T + 1$ sections as $S_k = \{S_0, S_1 \dots \dots S_k\}$. Where, T is chosen from threshold collection $T = \{t[r], t[r + 1], \dots \dots t[r + 1] - 1\}$; Each set is segmented from greyscale level T .

The probability of weight and mean weight segmented from each greyscale levels η and S can be calculated as

$$ws_k = \sum_{i \in S_k} Pr ob_i \tag{4}$$

$$\eta = \sum_{i \in S_k} \frac{Pr ob_i \cdot \max\{i, g * \log(i)\}}{ws_k}; g \in GC \tag{5}$$

Weighted mean greyscale intensity μ_{W1} and mean inter-class variance σ_{VS}^2 between the segments of the whole

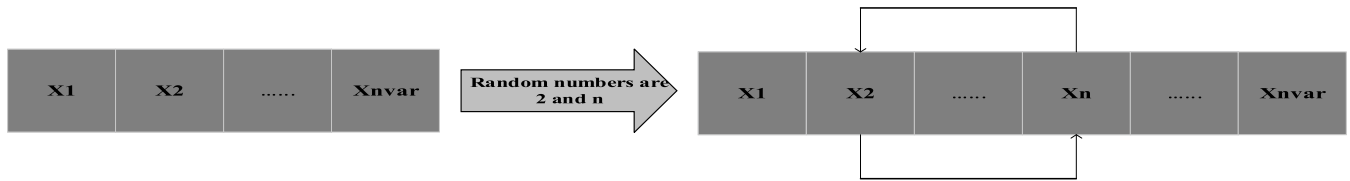


FIGURE 2. Mutation.

image is given by

$$\mu W1 = \sum_{i=0}^{\rho} i * Pr ob_i \tag{6}$$

$$\sigma_{VS}^2 = \sum_{i=0}^{\rho} w_{sk} \cdot \eta^2 - \mu_{W1}^2 \tag{7}$$

$$(\sigma_{VS}^2)* = \sum \max\{\sigma_{VS}^2(S_i), \sigma_{VS}^2(S_j)\} \tag{8}$$

The model determines the best thresholds for each grayscale of segmented area by maximizing variance of inter-class as much as possible.

$$\{t * [1], t * [2] \dots t * [n]\} \\ = argmax \sigma_{VS}^2 * (t [1], t [2] \dots t [T]) \tag{9}$$

To execute thyroid image segmentation, threshold technique is presented for automated image in this model. In the over-segmentation process, the inter-class variance between background and foreground intentions is evaluated, the noise level is estimated.

C. THYROID IMAGE FEATURE SELECTION USING HYBRID META-HEURISTIC ALGORITHM (BWO-MFO)

To prevent premature convergence and accelerate convergence speed, increase population diversity. As earlier discussed, the proposed model has associated with Vgg-19-LSTM with BWO and MFO. Here, the section mainly covers a hybrid Meta heuristic algorithm where the hybridization of Mayfly and Black Widow Optimization algorithm is discussed in detail. In Mayfly, it can gradually increase population diversity against premature convergence. In addition, it effectively enables the local optimum. The following section provides the mathematical models of the initial population procreation, cannibalism, mutation, and convergence is provided.

D. INITIAL POPULATION

In Black Widow Optimization (BWO) algorithm, the population is initially executed randomly, where two types of populations require such as male and female. Based on this initialization offspring are generated for the future generation. In this process, the computation of fitness value is significant; the fitness function is denoted as f at a widow. The following shows a mathematical representation of the black

widow spider’s initial population.

$$X_{N,d} = \begin{bmatrix} x_{1,1} & x_{1,2} & x_{1,3} & \dots & x_{1,d} \\ x_{2,1} & x_{2,2} & x_{2,3} & \dots & x_{2,d} \\ x_{N,1} & x_{N,2} & x_{N,3} & \dots & x_{N,d} \end{bmatrix} \\ lb \leq X_i \leq ub \tag{10}$$

$x_{N,d}$ is the black widow spider’s population, N indicates population size, d denotes the number of decision variables of the problem, lb is the population lower bound, and ub is the population upper bound. The potential solution populations $x_{N,d}$ are utilized for minimizing or maximizing the following objective function represented in Equation (2):

$$RMSE = \frac{1}{n} \sum_{i=1}^n w_i(t_i - \hat{t}_i)^2 \tag{11}$$

N –total count of samples

t_i - True sample value

\hat{t}_i - Corresponds to the predictive value

E. PROCREATE

Each pair is independent in the group where they parallelly act for mating to produce a new generation. As discussed, they individually process mating in the web from other spiders. Therefore, in the real-time process, they produced 10K eggs approximately. However, the fittest spider or strongest spider in the web only survives. In this algorithm, an array is considered for the reproduction process, this array-based reproduction is carried out until a widow array with random numbers is available. Then, μ is denoted for creating an offspring based on the following equation,

x_1 and $x_2 \rightarrow$ Parents

y_1 and $y_2 \rightarrow$ Offspring

$$y_1 = \mu \times x_1 + (1 - \mu) \times x_2 \tag{12}$$

$$y_2 = \mu \times x_2 + (1 - \mu) \times x_1 \tag{13}$$

i and j can be represented in the range of 1 to N

μ can be determined in the random range of 0 and 1. Cc

F. CANNIBALISM

Cannibalism can be executed by three types such as sexual cannibalism, Child cannibalism, and sibling cannibalism. In sexual cannibalism, the male spider is eaten by the female while mating or after mating. Here, fitness value is highly considered in this process. The second cannibalism is child eats their parents based on their fitness value to determine the

spiderlings are weak or strong. Likewise, sibling cannibalism is spider eats its sibling if it is weak. In this algorithm, the cannibalism rate is determined for computing the survivor rate.

G. MUTATION

The mutation process is executed based on the random selection process for producing the population by selecting the Mute pop number. Figure 2, the two elements in the array at random to be exchanged based on the chosen solution. The mutation rate is used to calculate mute pop.

H. CONVERGENCE

To increase population diversity, premature convergence is to be prevented; convergence speed needs to be accelerated with the Mayfly optimization algorithm. The mayfly has the unique properties of increasing population diversity sequentially. This process helps to come out from the local optimum. Moreover, this method is efficient for the exploration and exploitation process using MFO.

Here, the convergence process of modified Mayfly optimization algorithm is incorporated based on applying equation (5). The mathematical formulation of the process is shown below.

$$X_i^{i+1} = X_i^i + usign[rand - 0.5] \oplus Levy(\beta) \quad (14)$$

where, $X_i^{i\text{th}}$ → Solution vector or mayfly,
 X_i → No of iteration,
 t, u → Random parameter is considered for uniform distribution
 \oplus → Dot product (entry wise multiplications)
 $rand$ → random initialization range is [0,1].

The representation is given with sign [rand - 0.5] where only 3 values can consider such as 0, 1, and -1. Likewise, the equation (5) has the combination of u sign [rand - 0.5] and the mayfly can execute the random walk. With this process, the local minima can be reduced, and global search capability can be improved with the incorporation Modified Mayfly in Black Widow Optimization process.

Moreover, the Mayfly process is mainly relying on random walk where step length helps to determine the step in its process, and the Levy distribution process is confirmed by the jumps process. The mathematical operation of this process is shown below.

$$Levy(\beta) \sim \mu = t^{-1-\beta}, (0 \leq \beta \leq 2) \quad (15)$$

The equation (6) is to compute the Levy random numbers.
 The equation (6) is to compute the Levy random numbers.

$$Levy(\beta) \sim \frac{\theta \times \mu}{|v|^{1/\beta}} \quad (16)$$

Where, μ and v → standard normal distributions
 Γ → a standard Gamma Function

$\beta = 1.5$, and ϕ is defined as follows:

$$\begin{aligned} &(\Gamma(1 + \beta) \times \sin(\pi \times \beta / 2) \\ &\times |\Gamma((1 + \beta)/2) \times \beta \times 2^{(\beta-1/2)}|)^{1/\beta} \quad (17) \end{aligned}$$

Here, the Global Search Ability of the proposed algorithm is improved by the incorporation of Random Walk with Levy-Flight to eliminate the weakness of MFO algorithm. With this process, local minimum process can be mitigated to generate the successful result especially multi-model benchmark functions and uni-model functions.

I. PSEUDO-CODE OF THE BWO-MFO

Input: Max- number of iterations, Number of cannibalism rate, procreate rate to num. of reproduction is “nr”, mutation rate

Output: Objective function’s –RMSE,
//Initialization

1. Initialize the population of BWO, D-dimensional problem, Chromosome’s D-dimensional array for each pop.
2. Fitness value (RMSE) evaluation until termination reached.
3. Determine nr and find the best solution in pop1 (population 1)

// Procreating and cannibalism

4. For i = 1 tonrdo
5. Choose two solutions at random as parents from pop1.
6. Using equation 1, generate D children.
7. Choose two solutions randomly as parents from pop1.
8. Equation 1 is considered for generating D children.
9. Do cannibalism to for destroying father and some weakest children and generate new solution.
10. Generate new pop2 based on remaining solution.
11. End for

// Updating

12. Modified-Mayfly optimization algorithm to update the population.
13. Return the best solution from pop;
14. The obtained best solution is given into the CNN-LSTM classifier. The obtained best solution is given into the CNN-LSTM classifier.
15. The performance is evaluated to prove the best classifier.
16. stop

J. THYROID DISEASE CLASSIFICATION USING VGG-19 WITH LSTM

There are several CNN models available now that have improved performance and deeper architecture. But deeper networks are more complex to train due to the requirement of huge range of data and immense parameters. The existence of a large-scale, exactly categorized dataset is critical for correct and generalizable frameworks. The block-wise architecture of the Vgg-19 is shown in figure.3.

In this paper, feature extraction process was carried out by the Vgg- 19 network which is pre-trained on Image Net.

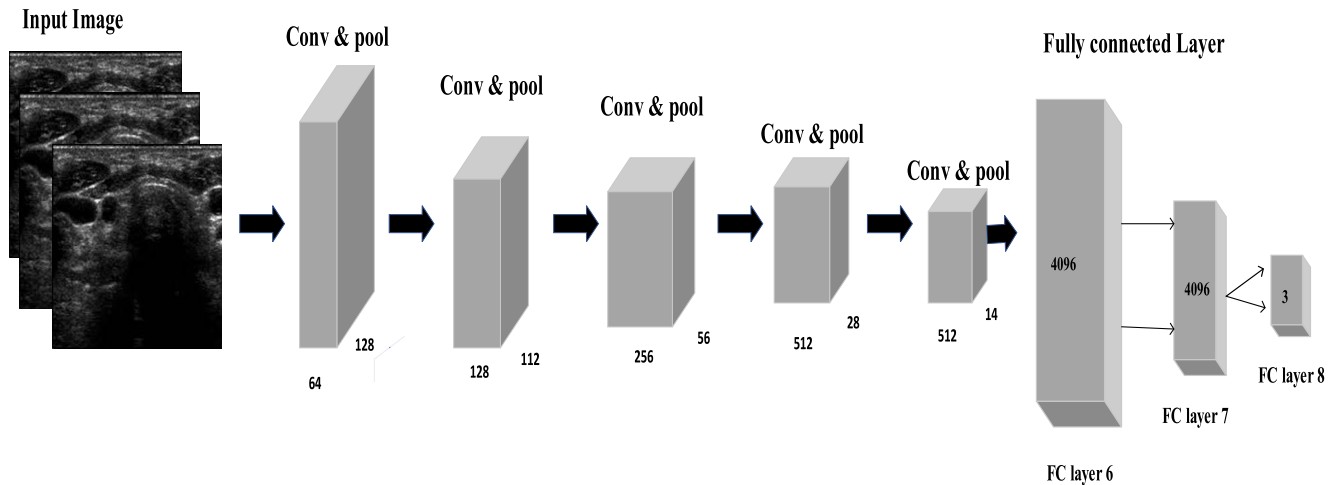


FIGURE 3. Vgg-19 architecture.

These features utilized as input signals for 1 LSTM layer. VggNet includes 16 convolutional layers with 3×3 filters with a stride of 1 in the convolutional layer, 5 max-pooling layers, 1 flatten and 3 fully connected (FC) layers. Vgg-19 has multiple stacked small size kernels in filters that improve the depth of the network which allows the network to extract difficult features at a lower cost.

A version of the normal RNN is the long short-term memory (LSTM) network. The LSTM network can better address the problem of gradient vanishing and expansion of long-term dependence by replacing the fundamental hidden neurons with LSTM units in RNN. LSTM has based three gates like an input, a “forget”, and also an output gate, here x_t represent the present input; c_t as well as c_{t-1} denote new & previous cell states, accordingly; h_t and h_{t-1} are current and previous outputs, respectively. The principle of the LSTM input gate is shown as follows.

$$i_t = \sigma(W_i \cdot [h_{t-1}, x_t] + b_i) \quad (18)$$

$$C'_t = \tanh(W_i \cdot [h_{t-1}, x_t] + b_i) \quad (19)$$

$$C_t = f_i C_{t-1} + i_t C'_t \quad (20)$$

Equation (24) is utilized to determine that the information portion is added by passing h_{t-1} and x_t through a sigmoid layer. After passing h_{t-1} and x_t through the \tanh layer, Equation (25) is employed to provide new data. Equation (26) associates the present moment data, C'_t , also long-term memory data, C_{t-1} & C_t , where W_i denotes a sigmoid output and C'_t denotes a \tanh output. Weight matrices describe W_i , while b_i denotes LSTM's bias input gate. A dot product and a sigmoid layer are utilized, the forget gate of LSTM's allows for select transmission of data. Equation (27), in where W_f determines the weight matrix, b_f is offset, and σ is the sigmoid function, is used to decide related information from the previous cell with specific possibilities.

$$f_t = \sigma(W_f \cdot [h_{t-1}, x_t] + b_f) \quad (21)$$

The states that determine the LSTM's output gate, required for continuation by h_{t-1} and x_t input in Equations (28), (29). State decision vectors, which passes new information, C'_t through \tanh layer is multiplied by the final output.

$$O_t = \sigma(W_o \cdot [h_{t-1}, x_t] + b_o) \quad (22)$$

$$h_t = O_t \tanh(C_t) \quad (23)$$

where W_o & b_o are weighted matrices output gate & LSTM bias, respectively.

To detect and classification thyroid disease using a lateral full thyroid ultrasound dataset, a hybrid algorithm and Vgg-19 - LSTM method were developed in this paper. This structure was created by hybrid optimization and LSTM networks, with extracting images' complex features and the LSTM serving as the classifier. Network layers: one layer of LSTM, two-layer of FC, and three dense layers based on activation function. One LSTM layer, tracked by 0.5 dropout rate. The ReLU function activates the convolutional with a size of 3×3 kernel which is employed for feature extraction. An input image dimensional is minimized, size of the max-pooling layer is utilized with a 2×2 kernel. The architecture organizes the ultrasound thyroid images through a completely interconnected layer after analyzing the timing features to predict whether they belong in one of two groups (normal and abnormal).

K. HYPER-PARAMETER TUNING WITH HYBRID (BWO-MFO)

Hyper-parameters selection is significant process of deep learning performance improvement; therefore, appropriate technique should consider for enhancing the tuning process. Especially, the tuning in complex architecture like LSTM is highly difficult. Thus, the reason, an incorporation of effective optimization makes tremendous impact in the performance of deep learning. Here, a hybrid meta-heuristic algorithm is considered including Black Widow and Mayfly optimization hybrid BWO. Moreover, the hybrid

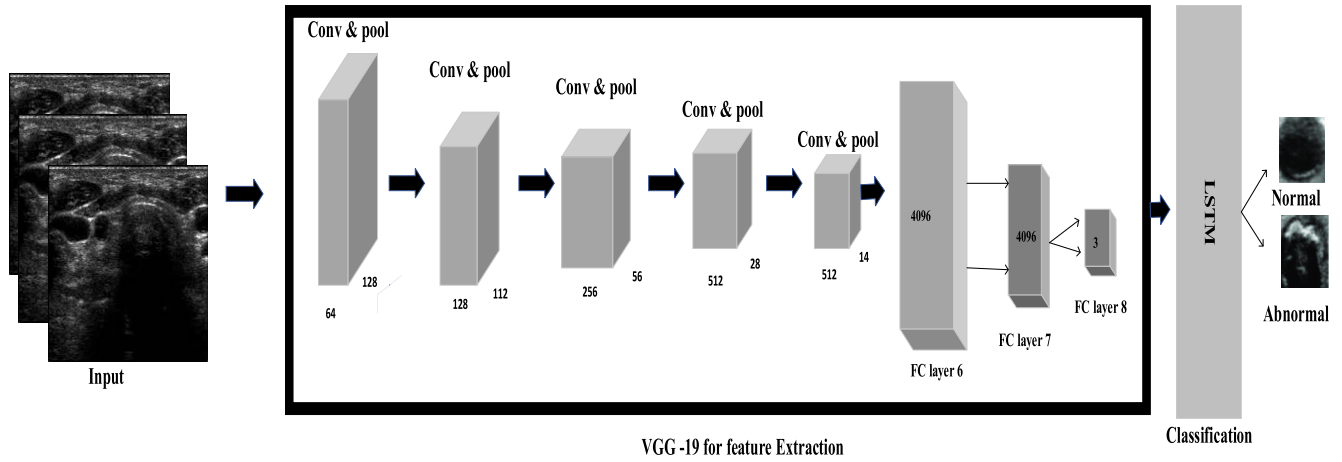


FIGURE 4. Classification structure.

BWO approach to solve optimization problems of selecting and tuning hyper-parameters makes huge difference than other optimizations. The reason behind the selection of hybrid BWO is to enhance the convergence speed of BWO.

The proposed algorithm, hybrid BWO, manages an overall population space, which is shared by BWO and MFO. To increase population diversity, premature convergence is to be prevented; convergence speed needs to be accelerated with the Mayfly optimization algorithm. This algorithm provides more convergence speed; therefore, the performance and outcomes can be attained in effectively. As the discussion in the previous section, LSTM model is enhanced through tuning the parameters of LSTM with the HM- BWO- strategy. Different parameters are used for this work that are Sequential Input Layer, LSTM Layer, Dropout Layer, Fully Connected Layer, and SoftMax Layers. The parameters utilized for this work are tabulated below. The major layers of vgg-19-LSTM are shown in Figure 8 shows the flowchart of the proposed work.

IV. EXPERIMENTAL RESULTS AND DISCUSSIONS

A. DATASET DESCRIPTION AND EVALUATION METRICS

In this analysis DDTI dataset (<https://www.kaggle.com/datasets/dasmehdixtr/ddti-thyroid-ultrasound-images?resource=download>) was utilized to detect the thyroid nodules which includes 99 cases and 134 images. The dataset was separated into two parts as 80% and 20% for training and testing progression. The duration for the training process was 102.93156 seconds and the duration required for recognize the thyroid nodules was 5.304 seconds. Moreover, the efficacy of the system is verified by comparing the performance metrics of the presented method with the existing methods. The ranges for the performance metrics are obtained through the confusion matrix. Here, Accuracy, Precision, Recall, F1_score, specificity, recognition time, training time, loss, FDR, FNR, FPR, MCC and NPV are considered as performance metrics for this experimental.

Accuracy: Accuracy can be distinct as, from the overall count of thyroid images, a percentage of the count of

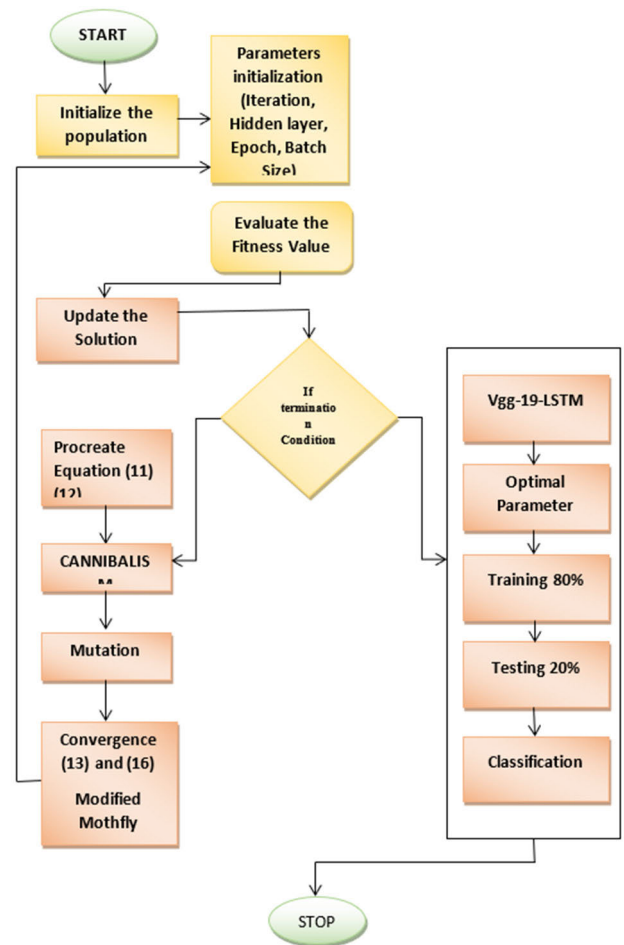


FIGURE 5. Flowchart of proposed Vgg-19 LSTM parameters.

accurately categorized thyroid images.

$$Accuracy = \left(\frac{(Tp + Tn)}{(Tp + Tn + Fp + Fn)} \right) \tag{24}$$

Precision: Precision is defined as the ratio of exactly classified positive thyroid images to the count of positively

forecasted thyroid images.

$$Precision = \left(\frac{Tp}{(Tp + Fp)} \right) \quad (25)$$

Recall: Recall can be defined as the ratio of exactly classified positive thyroid images from the count of positive thyroid images.

$$Recall = \left(\frac{Tp}{(Tp + Fn)} \right) \quad (26)$$

F1_Score: F1_Score is defined as the mean harmonic range between the precision and recall.

$$F1_{Score} = \left(\frac{2(Recall \times precision)}{Recall + precision} \right) \quad (27)$$

Specificity: Specificity is distinct as the ratio of exactly categorized count of negative thyroid images to the total count of negative thyroid images.

$$Specificity = \left(\frac{Tn}{(Tn + Fp)} \right) \quad (28)$$

FDR: FDR stands for False Discovery Rate. FDR can be defined as proportion of total count of false positively classified thyroid images to the total count of positively categorized thyroid images.

$$FNR = \left(\frac{Fn}{(Fn + Tp)} \right) \quad (29)$$

FPR: FPR is false-positive rate. FPR is the proportion of incorrectly categorized thyroid images as positive to count of negative thyroid images.

$$FPR = \left(\frac{Fp}{(Fp + Tn)} \right) \quad (30)$$

MCC: MCC is Matthew's Correlation Coefficient. MCC is a correlation coefficient computed via following values such as Tp , Tn , Fp , and Fn .

$$MCC = \left(\frac{((Tp \times Tn) - (Fp \times Fn))}{\sqrt{((Tp + Fp)(Tp + Fn)(Tn + Fp)(Tn + Fn))}} \right) \quad (31)$$

NPV: NPV stands for negative predictive value. NPV can be defined at any given threshold, the likelihood of true non-hit variations being correctly categorized as non-hits.

$$NPV = \left(\frac{Tn}{(Tn + Fn)} \right) \quad (32)$$

The investigational progression is accomplished at MATLAB Software on computer with 12 GB RAM, Intel (R)core (7M) i3-6100CPU @ 3.70 GHz processor. MATLAB code was used to formulate and train the LSTM as well as VGG-19 of Deep Learning (DL) framework and discover the hyperparameters by Black Widow Optimization as well as Mayfly Optimization Approach (HBWO-MOA).

B. RESULTS AND DISCUSSION

In this work, deep learning approach is combined with the meta heuristic algorithms namely (LSTM) and VGG-19 of deep learning with Black Widow Optimization as well as Mayfly Optimization Approach (HBWO-MOA) to effectively recognize the thyroid nodules. Here the features were selected by the hybrid optimization approach namely HBWO-MOA and thyroid nodules were classified and detected by the hybrid deep learning techniques namely LSTM_CNN with VGG19. The outcomes of the performance metrics exhibits the efficient level of the presented approach. Additionally, hypermeter is taken for this experimental namely such as 20as epoch, 32 as batch size and 0.06 as learning rate. Furthermore, different thyroid images are taken as an input from the open-source dataset to predict the thyroid nodule from given image.

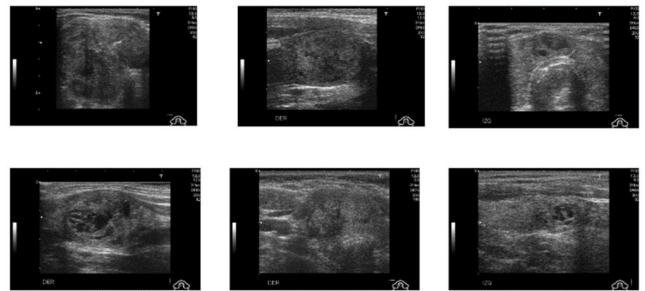


FIGURE 6. Sample images of thyroid nodules.

Figure 6 represents the input sample images taken for this analysis. These input images are pre-processed, segmented, and classified to detect whether there are thyroid nodules or not.

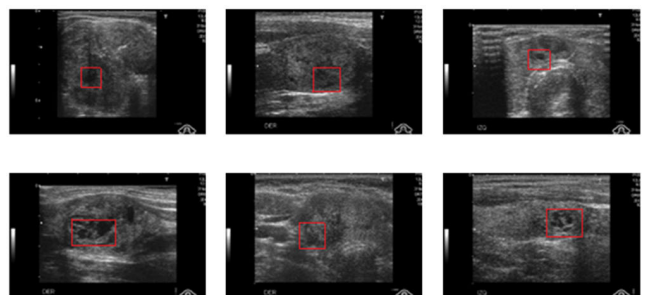


FIGURE 7. Detected thyroid nodule images.

The above figure 7 represents the detected portion of the thyroid nodule. The affected portion was displayed by the red color square box.

C. COMPARATIVE ANALYSIS FOR CLASSIFICATION AND PREDICTION

In this analysis, efficacy of the presented approach is validated by comparing it with the different existing approaches

such as convolutional neural network (CNN), ResNet50, Recurrent neural network (RNN), deep neural network (DNN).

TABLE 2. Overall performance of proposed model.

Techniques	ALEXNET	ResNet50	Vgg16 LSTM	Proposed Approach
Accuracy	89.4	81.4	85.9	98.8
Precision	84.89	76.9	78.62	99.2
Recall	92	81.4	89.4	96.56
F1_score	79	81.6	90	93.24
Specificity	78.6	78	88.9	89.16
Recognition time	7.325s	7.15s	6.459s	5.304 s
Training time	156.23s	123.621s	116.852s	102.93156 s
Loss	0.124	0.09	0.05	0.025
FDR	0.0289	0.042	0.022	0.024
FNR	0.0235	0.042	0.042	0.024
FPR	0.0218	0.042	0.052	0.034
MCC	0.465	0.242	0.552	0.641
NPV	0.521	0.542	0.252	0.934

By varying the learning percentage, detection of thyroid disease was accomplished by various measures through the ultrasound thyroid nodules images which is depicted in following figures. The presented method exhibits superior outcome than the existing methods.

The experimental analysis of the proposed method compared with other existing techniques, which is denoted graphically in Figure 8. In Figure: 8a, accuracy range for the proposed approach is much higher when compared with other existing approaches. At learning rate 60%, accuracy of proposed approach is 98.8 % which is better than other techniques. Moreover, the specificity of proposed approach is exactly detecting true-negative values from the false-positive values in Figure: 8e. Thus, specificity of proposed approach is 89.16% superior, when compared with other techniques. The precision of presented approach determined the positive values that are shown in Figure: 8b. This obtained as 99.2%. The overall performance of proposed model is tabulated in above Table. This may be the equivalent approach of State of The Art (SOTA) which uses DeciNets instead of other techniques.

NPV of endorsed Hybrid approach is 0.934 at a learning rate of 60% which is superior to other existing techniques and given in Figure: 8j. In Figure: 8i, MCC of proposed method is 0.614 at a learning rate of 60%. Furthermore, at learning rate of 60%, FDR of recommended Hybrid approach is 0.024 and it is given in Fig. 8f. From Fig. 8g and 5h, the FNR and FPR of the proposed method are 0.024 and 0.034 respectively at a learning rate of 60%. Finally, this is proved that the implemented hybrid approach is effective in predicting the thyroid disease.

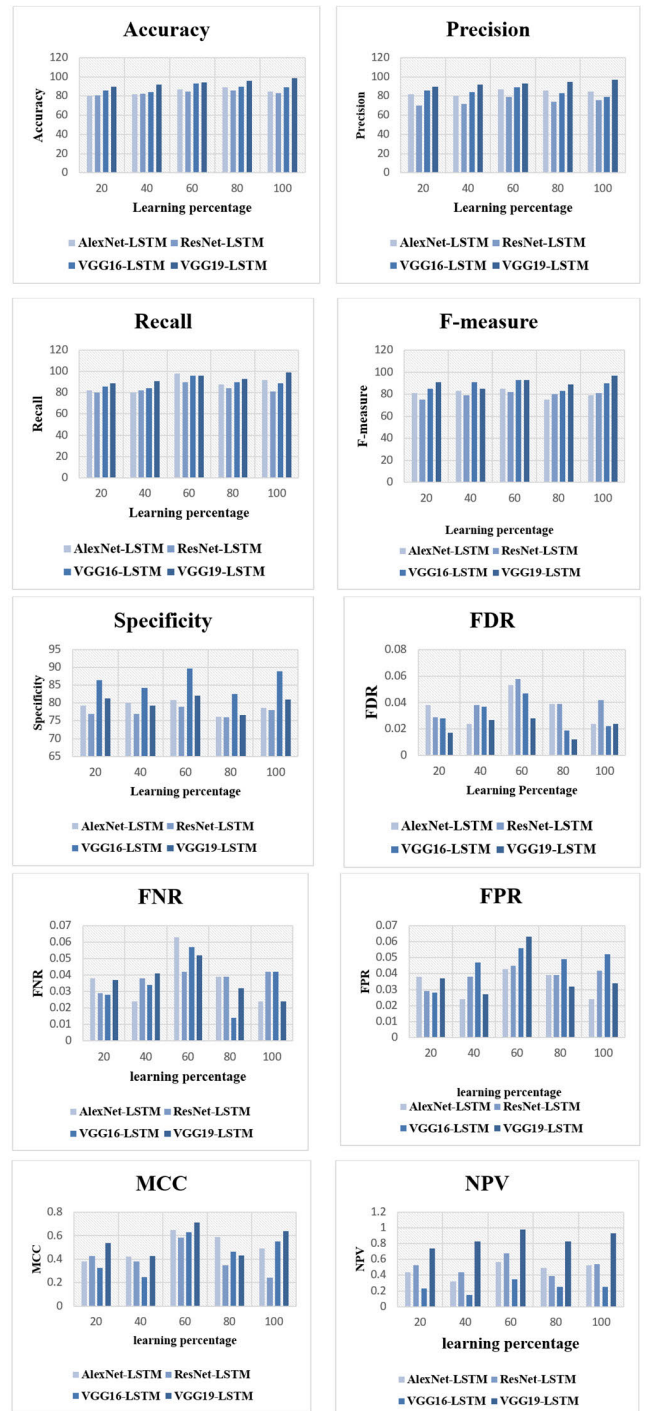


FIGURE 8. Graphical representation for comparative analysis.

V. CONCLUSION

The autonomous measuring of thyroid characteristics is the medical use of artificial intelligence is seen as a major future trend. To predict thyroid disease detection and classification, a unique DL approach was utilized in this research. Ultrasound images are taken in a sequence, and LSTM is providing more vision to absorb the sequences of this type of data.

Hence, the proposed method outperformed by utilizing the (Vgg-19-LSTM) model for thyroid disease recognition. To improve classification accuracy, large thyroid image information is required to determine normal or abnormal is the major issue. The high dimensional feature subset is essential to implement an accurate Deep Learning (Vgg-19-LSTM) with less error rate and time. Therefore, to enhance the level of prediction on thyroid image, pre-processing, segmentation, hybrid (BWO-MOA) optimization for feature selection, and (Vgg-19-LSTM) classifier is utilized in this work. For thyroid disease detection and classification, the proposed technique has better accuracy and high computational efficiency. In future, we will extend this work for classification task by designing a model that can accurately predict the pixel labels for a thyroid disease with a limited amount of training data.

REFERENCES

- A. A. Seyhan and C. Carini, "Are innovation and new technologies in precision medicine paving a new era in patients centric care?" *J. Translational Med.*, vol. 17, no. 1, pp. 1–28, Dec. 2019.
- I. U. Din, A. Almogren, M. Guizani, and M. Zuair, "A decade of Internet of Things: Analysis in the light of healthcare applications," *IEEE Access*, vol. 7, pp. 89967–89979, 2019.
- R. Boutaba, M. A. Salahuddin, N. Limam, S. Ayoubi, N. Shahriar, F. Estrada-Solano, and O. M. Caicedo, "A comprehensive survey on machine learning for networking: Evolution, applications and research opportunities," *J. Internet Services Appl.*, vol. 9, no. 1, pp. 1–99, Dec. 2018.
- A. Angelopoulos, E. T. Michailidis, N. Nomikos, P. Trakadas, A. Hatziefremidis, S. Voliotis, and T. Zahariadis, "Tackling faults in the industry 4.0 era—A survey of machine-learning solutions and key aspects," *Sensors*, vol. 20, no. 1, p. 109, Dec. 2019.
- D. Gupta, S. Sundaram, A. Khanna, A. E. Hassanien, and V. H. C. de Albuquerque, "Improved diagnosis of Parkinson's disease using optimized crow search algorithm," *Comput. Electr. Eng.*, vol. 68, pp. 412–424, May 2018.
- Y. Ito, A. Miyauchi, and H. Oda, "Low-risk papillary microcarcinoma of the thyroid: A review of active surveillance trials," *Eur. J. Surgical Oncol.*, vol. 44, no. 3, pp. 307–315, Mar. 2018.
- D. Grimm, "Cell and molecular biology of thyroid disorders," *Int. J. Mol. Sci.*, vol. 20, no. 12, p. 2895, Jun. 2019.
- Y. Zekri, F. Flamant, and K. Gauthier, "Central vs. peripheral action of thyroid hormone in adaptive thermogenesis: A burning topic," *Cells*, vol. 10, no. 6, p. 1327, May 2021.
- E. Fröhlich and R. Wahl, "Microbiota and thyroid interaction in health and disease," *Trends Endocrinol. Metabolism*, vol. 30, no. 8, pp. 479–490, Aug. 2019.
- T. J. Visser, "Regulation of thyroid function, synthesis, and function of thyroid hormones," in *Thyroid Diseases* (Endocrinology), P. Vitti and L. Hegedüs, Eds. Cham, Switzerland: Springer, 2018, doi: [10.1007/978-3-319-45013-1_1](https://doi.org/10.1007/978-3-319-45013-1_1).
- M. V. Deligiorgi and D. T. Trafalis, "The intriguing thyroid hormones–lung cancer association as exemplification of the thyroid hormones–cancer association: Three decades of evolving research," *Int. J. Mol. Sci.*, vol. 23, no. 1, p. 436, Dec. 2021.
- A. Abdel-Moneim, A. M. Gaber, S. Gouda, A. Osama, S. I. Othman, and G. Allam, "Relationship of thyroid dysfunction with cardiovascular diseases: Updated review on heart failure progression," *Hormones*, vol. 19, no. 3, pp. 301–309, Sep. 2020.
- Y.-T. Shen, L. Chen, W.-W. Yue, and H.-X. Xu, "Artificial intelligence in ultrasound," *Eur. J. Radiol.*, vol. 139, Jun. 2021, Art. no. 109717.
- M. Guo and Y. Du, "Classification of thyroid ultrasound standard plane images using ResNet-18 networks," in *Proc. IEEE 13th Int. Conf. Anti-Counterfeiting, Secur. Identificat. (ASID)*, Oct. 2019, pp. 324–328.
- S. Hassantabar, M. Ahmadi, and A. Sharifi, "Diagnosis and detection of infected tissue of COVID-19 patients based on lung X-ray image using convolutional neural network approaches," *Chaos, Solitons Fractals*, vol. 140, Nov. 2020, Art. no. 110170.
- T. Liu, Q. Guo, C. Lian, X. Ren, S. Liang, J. Yu, L. Niu, W. Sun, and D. Shen, "Automated detection and classification of thyroid nodules in ultrasound images using clinical-knowledge-guided convolutional neural networks," *Med. Image Anal.*, vol. 58, Dec. 2019, Art. no. 101555.
- L. Ma, C. Ma, Y. Liu, and X. Wang, "Thyroid diagnosis from SPECT images using convolutional neural network with optimization," *Comput. Intell. Neurosci.*, vol. 2019, pp. 1–11, Jan. 2019.
- R. Song, L. Zhang, C. Zhu, J. Liu, J. Yang, and T. Zhang, "Thyroid nodule ultrasound image classification through hybrid feature cropping network," *IEEE Access*, vol. 8, pp. 64064–64074, 2020.
- O. Moussa, H. Khachnaoui, R. Guetari, and N. Khlifa, "Thyroid nodules classification and diagnosis in ultrasound images using fine-tuning deep convolutional neural network," *Int. J. Imag. Syst. Technol.*, vol. 30, no. 1, pp. 185–195, Mar. 2020.
- F. Abdolali, J. Kapur, J. L. Jaremko, M. Noga, A. R. Hareendranathan, and K. Punithakumar, "Automated thyroid nodule detection from ultrasound imaging using deep convolutional neural networks," *Comput. Biol. Med.*, vol. 122, Jul. 2020, Art. no. 103871.
- B. Shankarlal, P. D. Sathya, and V. P. Sakthivel, "Computer-aided detection and diagnosis of thyroid nodules using machine and deep learning classification algorithms," *IETE J. Res.*, vol. 69, no. 2, pp. 995–1006, Feb. 2023.
- M. Hosseinzadeh, O. H. Ahmed, M. Y. Ghafour, F. Safara, H. K. Hama, S. Ali, B. Vo, and H.-S. Chiang, "A multiple multilayer perceptron neural network with an adaptive learning algorithm for thyroid disease diagnosis in the Internet of Medical Things," *J. Supercomput.*, vol. 77, no. 4, pp. 3616–3637, Apr. 2021.
- R. B. Namdeo and G. V. Janardan, "Thyroid disorder diagnosis by optimal convolutional neuron based CNN architecture," *J. Experim. Theor. Artif. Intell.*, vol. 34, no. 5, pp. 871–890, Sep. 2022.
- P. Wan, F. Chen, C. Liu, W. Kong, and D. Zhang, "Hierarchical temporal attention network for thyroid nodule recognition using dynamic CEUS imaging," *IEEE Trans. Med. Imag.*, vol. 40, no. 6, pp. 1646–1660, Jun. 2021.
- C. Chu, J. Zheng, and Y. Zhou, "Ultrasonic thyroid nodule detection method based on U-Net network," *Comput. Methods Programs Biomed.*, vol. 199, Feb. 2021, Art. no. 105906.
- A. Prasanth, P. Surendran, D. John, and B. Thomas, "A hybrid approach for web traffic prediction using deep learning algorithms," in *Proc. 9th Int. Conf. Electr. Electron. Eng. (ICEEE)*, Mar. 2022, pp. 383–386, doi: [10.1109/ICEEE5327.2022.9772575](https://doi.org/10.1109/ICEEE5327.2022.9772575).
- K. Bakhti and M. El Amin Larabi, "Comparing deep recurrent learning and convolutional learning for multi-temporal vegetation classification," in *Proc. IEEE Int. Geosci. Remote Sens. Symp. (IGARSS)*, Jul. 2021, pp. 4392–4395, doi: [10.1109/IGARSS47720.2021.9553175](https://doi.org/10.1109/IGARSS47720.2021.9553175).
- S. K. Prabhakar and S. Lee, "SASDL and RBATQ: Sparse autoencoder with swarm based deep learning and reinforcement based Q-learning for EEG classification," *IEEE Open J. Eng. Med. Biol.*, vol. 3, pp. 58–68, 2022, doi: [10.1109/OJEMB.2022.3161837](https://doi.org/10.1109/OJEMB.2022.3161837).
- D. S. AbdElminaam, N. Ahmed, M. Yasser, R. Ahmed, P. George, and M. Sahhar, "DeepCorrect: Building an efficient framework for auto correction for subjective questions using GRU_LSTM deep learning," in *Proc. 2nd Int. Mobile, Intell., Ubiquitous Comput. Conf. (MIUCC)*, May 2022, pp. 33–40, doi: [10.1109/MIUCC55081.2022.9781766](https://doi.org/10.1109/MIUCC55081.2022.9781766).
- E. E. Eryilmaz, D. Ö. Sahin, and E. Kiliç, "Filtering Turkish spam using LSTM from deep learning techniques," in *Proc. 8th Int. Symp. Digit. Forensics Secur. (ISDFS)*, Jun. 2020, pp. 1–6, doi: [10.1109/ISDFS49300.2020.9116440](https://doi.org/10.1109/ISDFS49300.2020.9116440).
- S. Iqbal, G. F. Siddiqui, A. Rehman, L. Hussain, T. Saba, U. Tariq, and M. A. Abbasi, "Prostate cancer detection using deep learning and traditional techniques," *IEEE Access*, vol. 9, pp. 27085–27100, 2021, doi: [10.1109/ACCESS.2021.3057654](https://doi.org/10.1109/ACCESS.2021.3057654).
- A. Sbrana, A. G. de Almeida, A. M. de Oliveira, H. S. Neto, J. P. C. Rimes, and M. A. C. Belli, "Plastic classification with NIR hyperspectral images and deep learning," *IEEE Sensors Lett.*, vol. 7, no. 1, pp. 1–4, Jan. 2023, doi: [10.1109/LESENS.2023.3234401](https://doi.org/10.1109/LESENS.2023.3234401).
- H. Jiang, M. Gao, H. Li, R. Jin, H. Miao, and J. Liu, "Multi-learner based deep meta-learning for few-shot medical image classification," *IEEE J. Biomed. Health Informat.*, vol. 27, no. 1, pp. 17–28, Jan. 2023, doi: [10.1109/JBHI.2022.3215147](https://doi.org/10.1109/JBHI.2022.3215147).



E. MOHAN received the M.E. degree in computer science engineering from Satyabhama University, the Ph.D. degree in computer science and engineering from Vinayaka Missions University, and the M.B.A. degree from Madras University. He has more than two decades of experience in the academic field. He is currently a Professor with the Saveetha School of Engineering, SIMATS, Chennai, Tamil Nadu, India. He titled three books and four scholars completed their Ph.D. under his guidance. Throughout his career, he is having good academic records of accomplishment and published in many refereed journals in reputed publications. His research interests include image processing, WSN, the IoT, ML, and data mining.



P. SARAVANAN received the M.C.A. and M.E. degrees from the Mailam Engineering College, Anna University, and the Ph.D. degree from Manonmaniam Sundaranar University, Thirunelveli. He has been with the Mailam Engineering College, since August 2011. He is currently an Assistant Professor with the SRM Institute of Science and Technology, Chennai. He has published ten national conferences, 13 international conferences, and 12 international journals.



BALAJI NATARAJAN received the Ph.D. degree (full-time) in computer science and engineering from Pondicherry University, Puducherry, India, in 2017. He has 15 years of teaching, research, and industry experience. He is currently a Professor and the Head of the Department of Computer Science and Engineering, Sri Venkateshwaraa College of Engineering and Technology, Ariyur, Puducherry. He has published more than 50 research papers in various reputed international journals and conferences. His research interests include web services, service-oriented architecture, evolutionary algorithms, artificial intelligence, and machine learning.



S. V. ASWIN KUMER received the degree in electronics and communication engineering from the Pallavan College of Engineering, Kanchipuram, in April 2008, the master's degree in embedded system technology from SRM University, Kanchipuram, in May 2012, and the Ph.D. degree for the implementation of image fusion using the artificial neural network from SCSVMV (Deemed to be University), Enathur, in February 2019. He is currently an Associate Professor with the Department of Electronics and Communication Engineering, Koneru Lakshmaiah Education Foundation (Deemed to be University), Guntur. He has more than 14 years of teaching experience. His research interests include digital communication and digital signal processing.



G. SAMBASIVAM (Member, IEEE) received the Ph.D. degree in computer science and engineering from Pondicherry University, Puducherry, India. He was the Dean of the School of Information and Communication Technology, ISBAT University, Uganda. He is currently an Assistant Professor with the School of Computing and Data Science, Xiamen University Malaysia, Sepang, Malaysia. His research interests include artificial intelligence, machine learning, deep learning, graph neural networks, web service computing, and soft computing techniques.



G. PRABU KANNA received the master's degree in information technology from the Kalasalingam Academy of Research and Education, India, in 2011, and the Ph.D. degree, in 2019. He has been in different academic and administrative roles in various institutions, since 2011. He is currently an Assistant Professor of Grade II with the School of Computing Science and Engineering, VIT Bhopal University, India. He has several publications, in peer-reviewed international and national journals with high-impact factors. He has contributed to a number of conferences, workshops, and faculty development programs. His research interests include cloud computing, big data, artificial intelligence, and machine learning.



VAIBHAV BHUSHAN TYAGI received the B.Tech. degree from UPTU Lucknow, in 2007, the M.Tech. degree from IIT Roorkee, in 2011, and the Ph.D. degree, in 2015. He is having more than 13 years of research and teaching experience around the globe. He is currently an Associate Professor (ECE) and the Dean of FICT, ISBAT University, Kampala, Uganda. He has worked in several administrative and academic positions in India, Ethiopia, and Uganda. His research interests include sensor applications in signal processing, signal modeling, artificial intelligence, and deep learning.

...